Journal of Sciences, Islamic Republic of Iran 26(2): 139 - 151 (2015) http://jsciences.ut.ac.ir
University of Tehran, ISSN 1016-1104

High-Pressure Marbles from the Nahavand Area in the Sanandaj-Sirjan Metamorphic Belt, Iran

J. Izadyar* and N. Skandari

Department of Geology, Faculty of Sciences, University of Zanjan, Zanjan, Islamic Republic of Iran

Received: 14 January 2015 / Revised: 4 February 2015 / Accepted: 17 February 2015

Abstract

Marbles containing high-pressure mineral assemblage was found from the Sanandaj-Sirjan metamorphic belt in the Nahavand area in western Iran. The high-pressure marbles occur as small bodies or lenses within pelitic schist layers and show compositional banding of carbonate- and silicate- rich bands. Textural analysis revealed two metamorphic stages. The early stage is testified by relicts of the minerals such as rounded jadeite-bearing diopside, epidote (clinozoisite), amphibole 1 (pargasite-edenite) and titanite 1. The second stage (main stage) documented to have phlogopite, chlorite, amphibole 2 (tremolite) and titanite 2. P-T-XCO2 estimates for the early stage of metamorphism give an average pressure, temperature and XCO2 of 13.5 kbar, 670 ºC and 0.35, whereas the second stage has been constrained at P=3.8 kbar, T=500 ºC and XCO2=0.45. The high-pressure mineral assemblage documented in the Nahavand area, were formed during the subduction stage, while the second metamorphic blastesis were recorded during the exhumation event.

Keywords: High-pressure metamorphism; Nahavand; Sanandaj-Sirjan; Marbles.

Introduction

High-pressure metamorphic terrains almost invariably include marbles of different types; yet the high-pressure paragenesis of these is poorly known. A few parageneses in marbles under eclogite facies conditions have been studied where high-pressure subduction metamorphism has developed under essentially static conditions and where the eclogite-bearing terrain has behaved as a coherent unit [7]. This is the case in the Triassic-Jurassic stratigraphic succession of the Tauern Window, Austria [16,42,10], where a carbonate sequence with different types and amounts of impurities underwent uniform conditions of eclogite facies metamorphism (T=600ºC, P=20 kbar). The most significant well preserved parageneses occur in siliceous dolomite, which have been transformed into marbles carrying the assemblage: calcite + dolomite + zoisite + tremolite + quartz; dolomite + zoisite + kyanite + quartz + phengite; calcite + dolomite + zoisite + quartz + phengite. Other impure marbles contain in addition a variety of silicate phases such as omphacite, epidote, Al-rich titanite and paragonite as well as non-silicate such as ankerite, magnesiosiderite and pyrite [17]. The assemblage found in the Tauern impure dolomitic marbles compare well with those of similar rocks in the Adula nappe prograde sequence [19], as well as in the eclogite-bearing terrains of Sifnos [30] and the western Alps. Here, however, the most

* Corresponding author: Tel: +982433054030; Fax: +982433054002; Email: izadyar@znu.ac.ir

common assemblage is calcite+dolomite+ankerite with scattered omphacite, garnet, phengite, glaucophane, zoisite, chloritoid and titanite [9,33,8]. Ye and Hirajima [46] show that impure marbles in eastern Shandong province of China, have been formed under high-pressure condition in early stage of metamorphism, contain zoisite, jadeite-bearing diopside and high-Al titanite. On the other hand, there are several evidences of high-pressure metamorphism in different parts of the Sanandaj-Sirjan metamorphic belt, for example, Davoudian et al. [12] reported eclogite in north of Shaherkord that experienced a pressure up to 24 kbar and in the same area Izadyar et al. [28] show that quartz schists in the Chadegan metamorphic complex, recorded a high-pressure metamorphism. Also, in the Nahavand area in western Iran, an unusual assemblage of talc, phengite, chlorite, K-feldspar was found in quartz schists that is the stable mineral assemblage in high-pressure metamorphic condition [27]. Agard et al.[1], studying blueschist in the Hajiabad area, estimated a high-pressure condition for the majority of blueschists and even documented apressure up to 18 kbar for some exotic blocks in serpentinite matrix. Even though, marbles are aboundant in different parts of the Sanandaj-Sirjan metamorphic belt, but their high-pressure mineral assemblage did not studied in detail. During a petrological investigation in the Nahavand area of the Sanandaj-Sirjan metamorphic belt, a high-pressure mineral assemblage in marbles was recognized. This paper is the first to describe the assemblage, to characterize its mineralogy and texture and to explain its P-T-X_{CO2} stability.

Geological setting

The Sanandaj-Sirjan metamorphic belt, which is 1500km long and up to 200km wide, stretches from the northwest to the southwest of Iran and is located between the central Iran block and Zagros Fold-thrust belt [43,5,2](Fig. 1A). The Sanandaj-Sirjan metamorphic belt consists of mafic-ultramafic rocks,

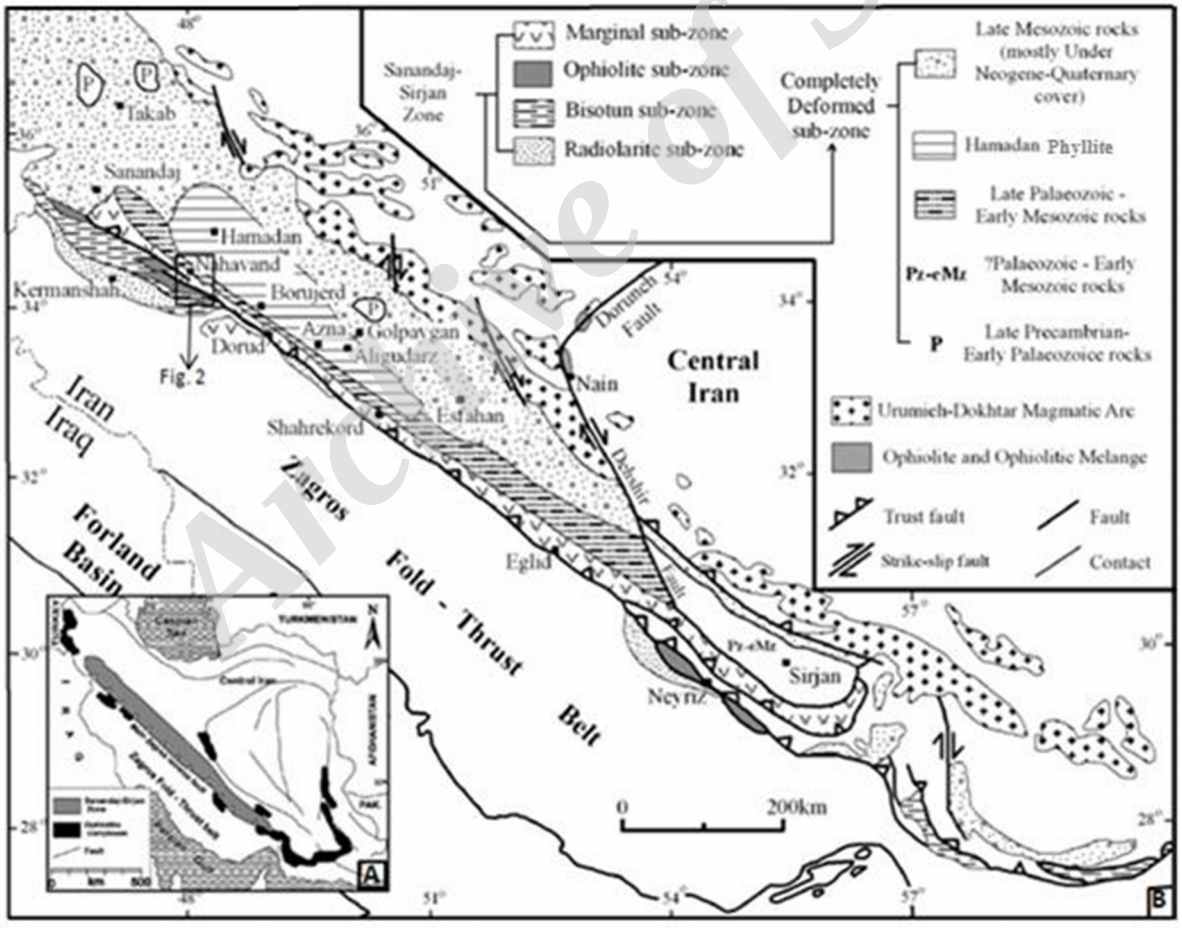

Figure 1. (A) Simplified structural map of Iran showing the location of the Sanandaj-Sirjan zone. (B) Tectonic map of southwestern Iran showing the divisions of the Sanandaj-Sirjan metamorphic belt (modified after Mohajjel et al.[32]).

metamorphic complexes and Paleozoic-Mesozoic sequences that underwent amphibolite/greenschist facies metamorphism during the Cretaceous-Tertiary continental collision between the Afro-Arabian continent and the Iranian microcontinent [39,31,32]. From the southwest to the northeast it consists of several elongated sub-zones (Fig. 1B) including radiolarite, Bisotun, ophiolite, marginal and complexly deformed sub-zones [32]. The last sub-zone is distinguished from the other sub-zones by abundant metamorphic rocks.

The Nahavand area belongs to the complexly deformed sub-zone and is located near the main Zagros reverse fault, which is proposed as a suture zone between the Arabian plate and Eurasia [38,1,18](Fig. 1B). Apart from a thin ophiolite unit, the lithologic units in the Nahavand region can be generally subdivided into two groups of metamorphosed and non-metamorphosed rocks [3](Fig. 2). The metamorphic rocks include five different successions that are in fault contact with both the overlying and underlying rocks. The oldest one (PTrm) is a sequence of massive marbles

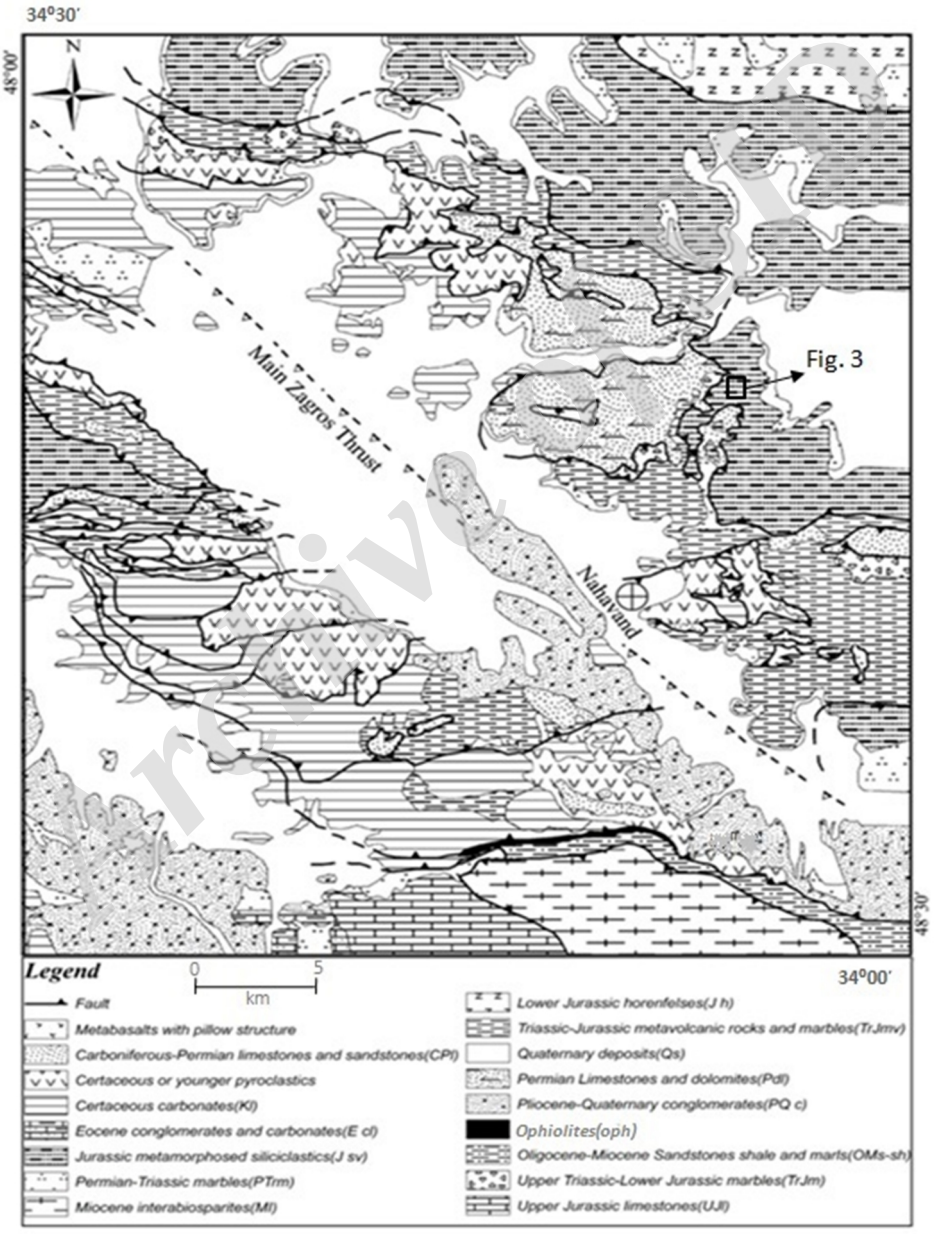

Figure 2. Geological map of the Nahavand area (modified after Alavi and Mahdavi [3]).

of Permian-Triassic age that are strongly sheared and mylonitized near the contact with the underlying rocks. The next succession (TrJmv) consists of an assemblage of Middle to Upper Triassic-Lowermost Jurassic metamorphosed basaltic and andesite-basaltic lava flows (with tholeitic affinities). This assemblage contains locally occurring pillow structures interlayered with well-foliated marbles that have thin, upward increasing slate layers. Small plutons of gabbro and diorite (now metamorphosed) have locally intruded this assemblage [3] (Fig. 2). The third unit (TrJm) consists entirely of a sequence of fossiliferous marbles of Late Triassic to Early Jurassic. The fourth succession (Jsv) is a sequence of Lower Jurassic slates, phyllites and metagreywakes that have intercalations of marbles and metamorphosed volcanic rocks in the lower parts. The fifth lithological unit (Jh) consists of an Upper Liassic succession of cordierite-bearing hornfels which is the product of contact metamorphism due to the intrusion of Late Cretaceous granitoid plutons [3](Fig. 2).

Materials and Methods

Mineral chemistry was acquired by a Cameca SX50 electron microprobe equipped with three wavelength dispersive spectrometers at Toronto University, Canada. The accelerating voltage and the beam current were maintained at 15 kv and 10 nA, respectively. Corrections were made using either the ZAF or Phi-Rho-Z method following Armstrong [4]. The structural formulae, the Fe^{3+}-content and end-member activities of the minerals were recalculated using the AX program of Holland and Powell (www.esc.com.ac.uk/pub/minp/AX). The mineral abbreviations are from Whitney and Evans [47].

Results

Petrogarphy

Marbles were collected from the Jsv unit that is a lower Jurassic sequence mostly of pelite and graywake origion (Fig. 3). This sequence usually occurs in the northwest of the Nahavand region. The marbles form 10-30 m thick layers interbedded with 100-150 m thick

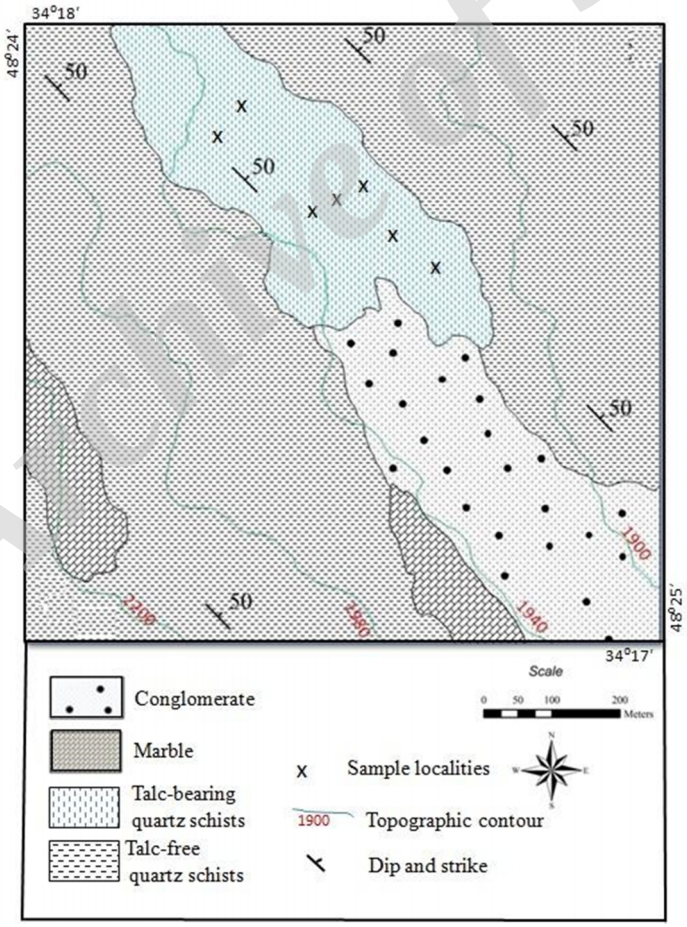

Figure 3. Lithological map of the studied area and sample localities.

Table 1. Mineral assemblages of high-pressure and common marbles from the Nahavand area.

Mineral Na.	Cpx	Ep	Amp	Ttn	Chl	Phl	Pl	Cal	Do
C122	+	+	+	+	+	+	+	+	+
C124	+	+	+	+	+	+	+	+	+
C126	+	+	+	-	+	-	+	+	+
C127	+	+	+	+	+	-	+	+	+
C128	-	-	+	-	+	+	-	+	+
C129	-	-	+	+	+	+	+	+	+
C130	-	-	-	-	+	+	-	+	+
C131	-	-	+	+	+	+	+	+	+

The mineral abbreviations are from Whitney and Evans (2010). Symboles (+) and (-) indicate present and absent minerals respectively.

politic schists and 30-50 m thick quartz schists. The marbles also occur as small bodies or lenses from one centimeter up to a maximum of three meters within politic schists layers. The high-pressure mineral assemblage could only be found in the marbles occurring as small bodies or lenses within pelitic schists. Therefore, based on the field and mineral assemblage, two types of marbles are recognized in the studied area which are named high-pressure and common marbles. The mineral parageneses of these two marbles are tabulated in Table 1. The high-pressure marbles contain coarser grains than common marbles and usually show compositional banding of carbonate-rich and silicate-rich bands (Fig. 4A). The width of the carbonate-rich bands ranges from 1 to 2 mm, and they are mainly composed of calcite, dolomite and subordinate amounts of silicate minerals (Fig. 4A). The silicate-rich bands mostly contain amphibole, pyroxene, epidote, chlorite and phlogopite with minor amounts of quartz, calcite and dolomite. The width of these bands

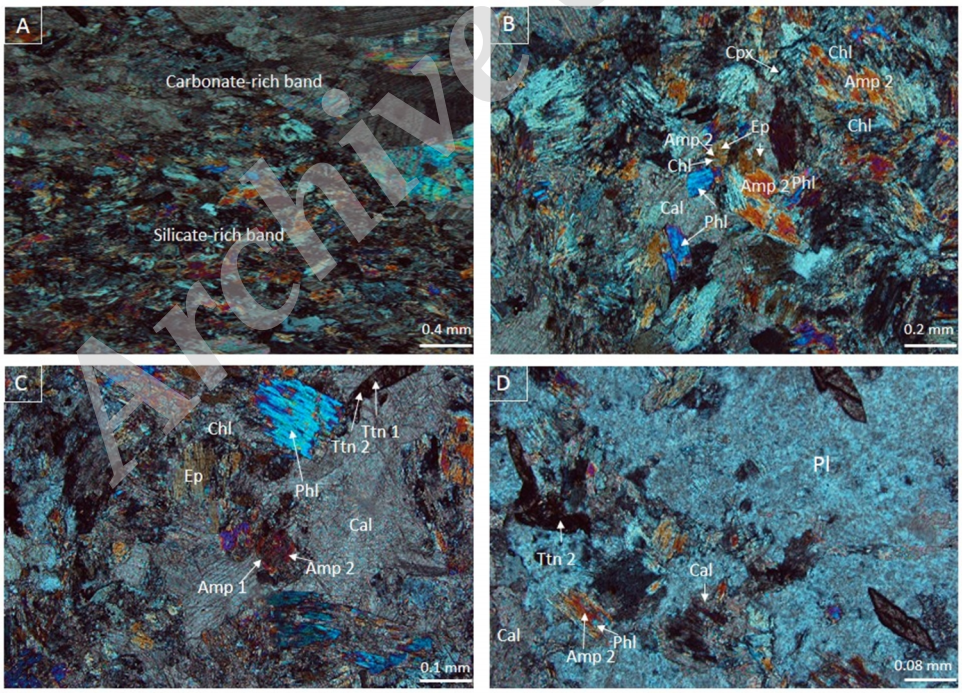

Figure 4. Photomicrographs of high-pressure marbles showing (A) carbonate-richand silicate-rich bands; (B) Rounded pyroxene and epidote that are decomposed to chlorite and amphibole 2. Phlogopite, chlorite and amphibole 2 coexistence; (C) titanite 1 is surrounded by titanite 2. Coexistence of phlogopite, calcite and amphibole 2; (D) Porphyroblast of plagioclase with titanite 2, amphibole 2 and phlogopite inclusions in its rim. Crossed polars. Abbreviations are from Whitney and Evans [47].

Table 2. Representative microprobe analyses of pyroxene (Cpx) and epidote (Ep).

Mineral Na.	Cpx				Ep			
Point No.	C1	C2	C4	C7	E1	E2	E3	E4
SiO_2	55.28	55.01	55.61	55.48	41.08	41.32	40.78	40.58
TiO_2	0.09	0.08	0.13	0.10	0.20	0.13	0.09	0.12
Al_2O_3	2.33	2.31	2.38	2.28	31.52	31.87	32.21	32.81
FeO	0.43	0.40	0.27	0.38	-	-	-	-
MgO	16.21	16.02	16.12	15.86	0.75	0.66	0.41	0.31
CaO	24.61	24.28	24.12	24.20	24.78	25.06	24.89	25.12
Na_2O	1.98	2.01	2.00	2.12	-	-	-	-
Total	100.93	100.11	100.63	100.42	98.33	99.04	98.38	98.94
Atom site	O=6				O=12.5			
Si	1.98	1.98	1.99	1.99	3.10	3.10	3.08	3.05
Ti	0.00	0.00	0.00	0.00	0.01	0.01	0.01	0.01
Al	0.98	0.10	0.10	0.10	2.81	2.82	2.87	2.90
Fe^{3+}	0.01	0.01	0.01	0.01	-	-	-	-
Fe^{2+}	0.00	0.00	0.00	0.00	-	-	-	-
Mg	0.86	0.86	0.86	0.85	0.05	0.04	0.03	0.02
Ca	0.94	0.94	0.92	0.93	2.01	2.02	2.01	2.02
Na	0.14	0.14	0.14	0.15	-	-	-	-
Total	4.00	4.03	4.02	4.03	7.98	7.98	7.99	8.00

The structural formula and Fe^{3+}-content recalculated with the AX program of Holland and Powell.

ranges from 1 to 2 mm and within them foliation and lineation are more visible (Fig. 4A). Pyroxene and epidote, usually, occur as rounded grains decomposed to amphibole and chlorite or surrounded by the minerals such as calcite, dolomite, phologopite and chlorite (Fig. 4B). Two different types of titanite are distinguished: titanite 1 occurs as rounded grains with discontinuous rim of titanite 2 (Fig. 4C). These textures indicate that the rounded pyroxene, epidote and titanite 1 are relicts of early stage metamorphism. Two different types of amphiboles are also identified: The first type, amphibole 1, is partially replaced by chlorite or surrounded by amphibole 2. The second type, amphibole 2, was found intergrown with chlorite and phologopite or as replacement of the rounded pyroxene grains (Figs. 4B and C). Phologopite occurs intergrown with chlorite and amphibole 2 but the rim of some phologopite is also decomposed to chlorite (Figs. 4B and C). Therefore, it is assumed that phologopite occurs in both early and main stage of metamorphism. The rim of plagioclase poikiloblast contains calcite, titanite 2, amphibole 2 and phlogopite that indicates its rim could be formed during the main stage of metamorphism (Fig. 4D).

By using the mentioned textural relationships, two different metamorphic stages can be distinguished:

Early stage: pyroxene, epidote, titanite 1, plagioclase 1, amphibole 1, calcite, dolomite, phologopite.

Main stage: amphibole 2, titanite 2, plagioclase 2, chlorite, phlogopite, calcite, dolomite.

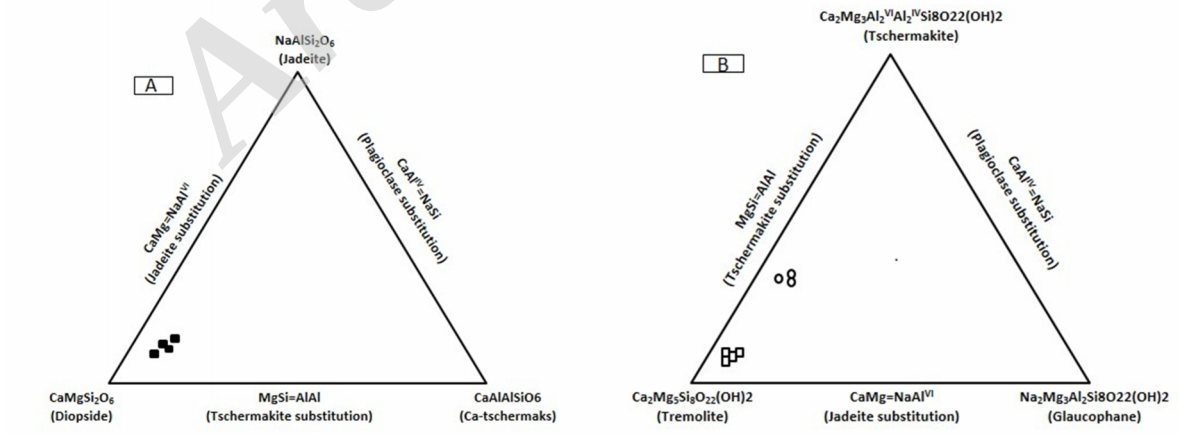

Figure 5. Substitutional diagrams showing the chemical compositions of pyroxene (A) and amphibole (B). Open square = amphibole 2. Open circle = amphibole 1. Filled square = Pyroxene.

Mineral chemistry

Pyroxene is rounded and its rim partly replaced by amphibole and chlorite, suggesting that pyroxene is a first stage mineral. Chemical analyses show that pyroxene composition is close to the ideal diopside end-member (Table 2). Deviation from ideal diopside end-member composition comes from jadeite (CaMg= $NaAl^{VI}$) and tschermak ($MgSi=Al^{IV}Al^{VI}$) substititutions. The deviation caused up to 12% jadeite and to 8% Ca-tschermak end-members to present in mostly diopside composition of pyroxene (Fig. 5A).

Epidote was also considered as first stage mineral, because its rounded grains partially decomposed to amphibole and chlorite. Its chemical composition is close to ideal clinozoisite end-member with small deviation towards pistacite composition (Table 2).

According to the IMA classification scheme [29], the studied amphiboles are calcic of tremolite, pargasite and edenite compositions. The amphibole 1 that is partially replaced by chlorite has pargasite and edenite composition, whereas the amphibole 2 occurs intergrown with chlorite and phlogopite has tremolite composition. Amphibole included in plagioclase rim, usually is tremolite (Table 3) (Fig. 5B).

Table 3. Representative microprobe analyses of amphibole.

Mineral Na.	**Amp 1**			**Am 2**			**Am 2 in Pl rim**	
Point No.	A1	A2	A3	A4	A5	A6	A7	A8
SiO_2	48.61	47.53	47.32	57.61	57.81	58.10	58.01	57.93
TiO_2	0.11	0.13	0.15	0.09	0.02	0.07	0.31	0.21
Al_2O_3	10.33	12.98	13.23	0.41	0.5	0.46	0.58	0.61
FeO	3.85	3.78	4.01	2.01	1.98	2.14	2.17	1.67
MgO	18.61	18.21	17.58	22.75	23.12	22.96	22.94	23.01
CaO	12.01	11.98	12.31	12.88	13.51	13.67	13.24	12.91
Na_2O	2.31	2.28	3.21	0.16	0.18	0.21	0.43	0.32
K_2O	0.73	0.63	0.53	0	0	0	0.09	0.08
Total	96.56	97.52	98.34	95.91	97.12	97.61	97.77	96.74
Atom site	O=23							
Si	6.89	6.65	6.62	8.00	7.95	7.96	7.93	7.97
Ti	0.01	0.01	0.02	0.01	0.00	0.01	0.03	0.02
Al	1.73	2.14	2.18	0.07	0.08	0.07	0.09	0.10
Fe^{3+}	0.04	0.14	-	-	-	-	-	-
Fe^{2+}	0.42	0.30	0.47	0.23	0.23	0.25	0.25	0.19
Mg	3.93	3.80	3.66	4.71	4.74	4.69	4.68	4.72
Ca	1.82	1.80	1.85	1.92	1.99	2.01	1.94	1.90
Na	0.64	0.62	0.87	0.04	0.05	0.06	0.11	0.09
K	0.13	0.11	0.10	-	-	-	0.02	0.01
Total	15.60	15.57	15.76	14.98	15.03	15.03	15.05	15.01

The structural formula and Fe^{3+}-iron recalculated with the AX program of Holland and Powell. Mineral abbreviations are from Whitney and Evans [47].

Table 4. Representative microprobe analyses of phlogopite.

Point No.	**phl1**	**phl2**	**phl3**	**phl4**	**phl5**	**phl6**
Loca.	-	-	-	-	Phl in Pl rim	
SiO_2	41.58	42.35	42.01	41.68	42.12	41.85
TiO_2	0.08	0.14	0.09	0.20	0.19	0.08
Al_2O_3	14.63	14.06	14.5	14.12	14.62	15.05
MgO	28.33	28.12	29.02	28.65	27.9	27.86
Na_2O	0.83	0.95	0.58	0.42	0.77	0.63
K_2O	9.01	8.97	9.03	9.00	9.02	9.03
Total	94.46	94.59	95.23	94.07	94.62	94.5
Atom site	(O=11)					
Si	2.90	2.94	2.90	2.91	2.92	2.91
Ti	0.00	0.01	0.01	0.01	0.01	0.00
Al	1.20	1.15	1.18	1.16	1.20	1.23
Mg	2.98	2.91	2.99	2.98	2.89	2.89
Na	0.11	0.13	0.08	0.06	0.10	0.09
K	0.80	0.80	0.80	0.80	0.80	0.80
Total	7.96	7.94	7.94	7.93	7.92	7.92

The structural formula recalculated with the AX program of Holland and Powell. Mineral abbreviations are from Whitney and Evans [47].

Phlogopite coexists with amphibole 2 and chlorite and some of them are partially decomposed to chlorite. Both types of phologopites are mostly composed of phlogopite end-member (Table 4).

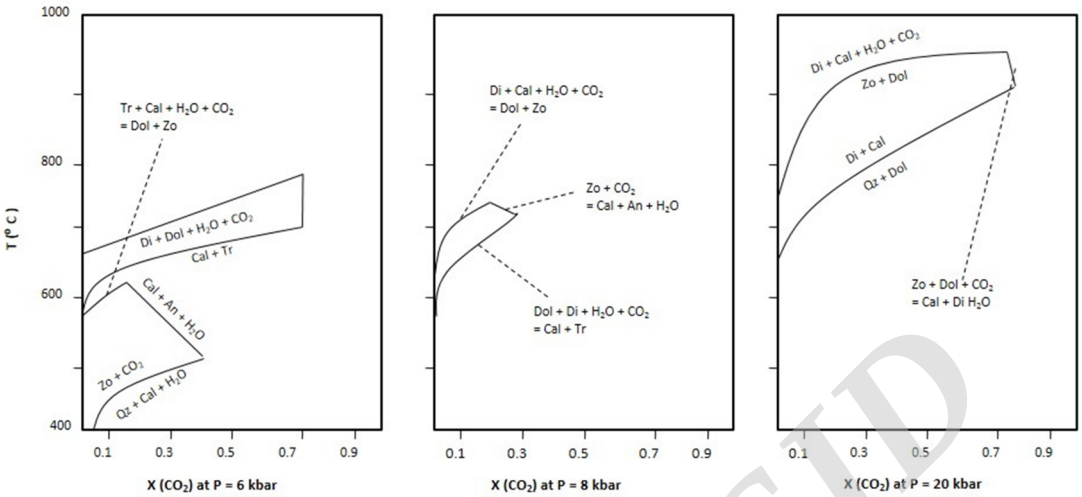

Figure 6. Stability relationships among dolomite, zoisite, diopside, calcite, quartz and fluid phases (H_2O-CO_2) in T-X_{CO2} diagrams: (A) P = 6 kbar; (B) P = 8 kbar; (C) P = 20 kbar. Abbreviations are from Whitney and Evans [47]. Modified after Ye and Hirajima [46].

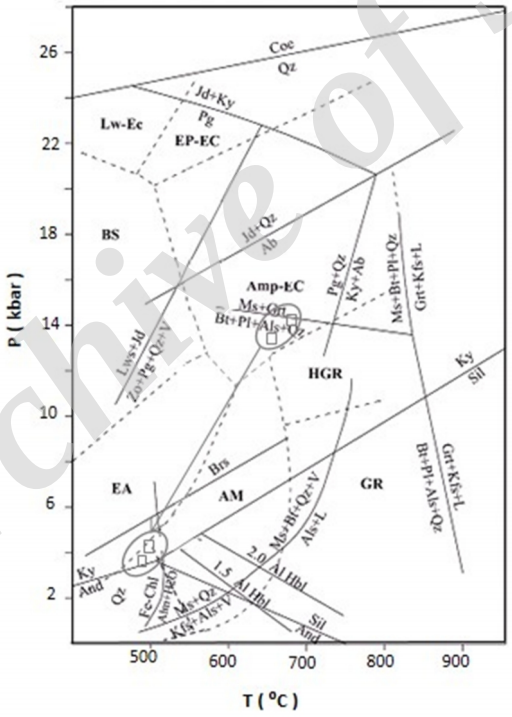

Figure 7. Petrogenetic gird and P-T paths for the marbles in the Nahavand area. Rectangles show P and T estimates obtained for M1 and M2 metamorphic events. The black arrows indicate P-T path for the marbles. Ab = Jd + Qtz after Holland [23]. Hornblende Al_{tot} contents are after Plyusnina [37]. Aluminium silicate triple-point according to Holdaway [21]. Coesite = quartz curve after Bohlen and Boettcher [6]. Barroisite stability field after Ernst [13]. Reactions Ms + Qz = Kfs + Als + V and Ms + Bt + Qz + V = Als + L are after Vielzeuf and Holloway [44]. Reactions Ms + Grt = Bt + Pl + Als + Qz and Ms + Bt + Pl + Qz = Grt + Kfs + L and Bt + Pl + Als + Qz = Grt + Kfs + L are after Vielzeuf and Schmidt [45]. Reactions Jd + Ky = Pg and Pg + Qz = Ky + Ab from Holland [22]. Reaction Fe-Chl + Qz = Alm + H_2O after Hsu [26]. Reaction Lws + Jd = Zo + Pg + Qz + V from Heinrich and Althaus [20]. The background petrogenetic grid is from Ernst [15]. Metamorphic-facies abbreviations are: AM = amphibolite; Amp-EC = amphibolite-eclogite; BS = blueschist; EA = epidote amphibolite; Ep-EC = epidote-eclogite; GR = sillimanite-granulite; HGR = kyanite-granulite; Lw-EC = lawsonite-eclogite. Mineral abbreviations for names are from Whitney and Evans [47].

Table 5. Representative microprobe analyses of titanite.

Point No.	Ti 1	Ti2	Ti3	Ti4	Ti5	Ti6
Loca.	core	rim	core	rim	Ttn in Pl rim	
SiO_2	31.54	31.9	31.23	32.08	31.71	31.89
TiO_2	25.73	28.21	27.51	29.23	28.36	29.01
Al_2O_3	10.52	8.31	9.42	8.41	8.75	8.62
MgO	0.23	0.16	0.31	0.17	0.31	0.16
CaO	30.04	29.83	31.08	29.92	29.89	29.04
Total	98.06	98.41	99.55	99.81	99.02	98.72
Atom site	(O=5)					
Si	1.03	1.07	1.06	1.09	1.03	1.08
Ti	0.65	0.71	0.63	0.72	0.66	0.73
Al	0.36	0.24	0.33	0.21	0.33	0.2
Mg	0.01	0.01	0.02	0.00	0.02	0.01
Ca	1.07	1.07	1.10	1.05	1.09	1.06
Total	3.12	3.10	3.14	3.07	3.13	3.08

The structural formula recalculated with the AX program of Holland Mineral abbreviations are from Whitney and Evans [47].

Table 6. Representative microprobe analyses of calcite (Cal) and dolomite (Dol).

Point No.	Ca1	Ca2	Ca3	Ca4	Dol1	Dol2
Loca.	core	core	rim	rim	-	-
FeO	0	0	0.31	0.28	0.44	0.31
MnO	0	0	0.23	0.64	0	0
MgO	0.63	0.71	0.82	0.90	20.92	21.75
CaO	52.12	51.84	53.1	52.45	30.31	29.83
CO_2	42.51	42.63	42.01	42.14	45.42	44.54
Total	95.26	95.18	96.47	96.41	97.09	96.43
Fe^{2+}	0	0	0.01	0.01	0.01	0.01
Mn^{2+}	0	0	0.01	0.02	0	0
Mg	0.03	0.04	0.04	0.05	0.97	1.00
Ca	1.97	1.96	1.94	1.93	1.02	1.99
Mg/Mg+Ca	0.02	0.02	0.02	0.03	0.32	0.33

The structural formula and Fe^{2+}-iron recalculated with the AX program of Holland and Powell.

Titanite 1 is rounded grain and contains extremely high-Al-content and has titanite 2 rim with lower Al than the core (Table 5). The high Al-content of titanite, possibly is accompanied with increasing of F and OH [46]. Smith [40] also show that Al, F and OH can replace Ti and O in the octahedral chains of titanite.

Calcite is chemically zoned with some Fe and Mn in the rim but no Fe or Mn in the core. The Mg/Mg+Ca ratio in the calcite rim is also relatively lower than its core. Dolomite appears to be homogenous and mostly composed of dolomite end-member with a few deviation towards ankerite by Fe=Mg substitution (Table 6).

Chlorite is high-Mg chlorite and mainly composed of clinochlore end-member (Table 7).

Poikiloblasts of plagioclase show chemical zonation in which its core contains higher Na and lower Ca than the rim (Table 8).

Table 8. Representative microprobe analyses of chlorite.

Point No.	ch1	ch2	ch3	ch4
SiO_2	32.42	32.01	32.12	32.85
TiO_2	0.09	0.10	0.09	0.12
Al_2O_3	17.43	18.71	17.75	19.02
FeO	5.02	4.75	5.01	4.64
MgO	30.09	31.41	29.41	28.41
Total	85.05	86.98	84.38	85.04
Atom site	(O=14)			
Si	3.13	3.03	3.13	3.16
Ti	0.01	0.01	0.01	0.01
Al	1.99	2.09	2.04	2.15
Fe^{2+}	0.41	0.38	0.41	0.37
Mg	4.34	4.43	4.27	4.07
Total	9.87	9.92	9.85	9.76

The structural formula and Fe^{2+}-iron recalculated with the Ax program of Holland and Powell.

Table 8. Representative microprobe analyses of plagioclase.

Point No.	Pl1	Pl2	Pl3	Pl4
Loca.	core	rim	core	rim
SiO_2	65.21	65.46	65.71	65.41
Al_2O_3	19.75	19.83	20.76	21.36
CaO	10.53	12.92	10.13	11.31
Na_2O	5.12	2.20	3.14	2.01
Total	100.61	100.41	99.74	100.09
Atom site	(O=8)			
Si	2.87	2.88	2.89	2.87
Al	1.03	1.03	1.08	1.10
Ca	0.50	0.61	0.48	0.53
Na	0.44	0.19	0.27	0.17
Total	4.83	4.70	4.71	4.67

Discussion

In order to constrain the P and T conditions recorded by the marbles during early and main stages of metamorphic events, we defined microstructureal domains where mineral assemblage are close to metamorphic equilibrium. Microstructural investigations and mineral chemistry results indicate that marbles in the Nahavand area record two events of metamorphism. The older event (early stage) is testified by relicts of the minerals assemblage such as rounded pyroxene, epidote and titanite 1. On the other hand, the later event (main stage), documented to have phlogopite, chlorite, amphibole 2 and titanite 2.

Yei and Hirajima [46] studied the stability of mineral assemblage of zoisite, diopside, calcite and dolomite under different P-T-X_{CO2} and show that at pressure lower than 6 kbar, the assemblages of diopside + calcite+ dolomite and zoisite+ calcite + dolomite are stable rather than zoisite + dioside associated with both calcite and dolomite. In 6 kbar pressure, these two assemblages were separated by two reactions: tremolite + calcite + CO_2 = anorthite + dolomite + H_2O and diopside + dolomite + H_2O + CO_2 = tremolite + calcite (Fig. 6A). In 8 kbar pressure, the assemblage of zoisite + diopside + calcite + dolomite becomes stable by the reactions: calcite + diopside + H_2O + CO_2 = zoisite + dolomite; zoisite + CO_2 = anorthite +calcite +H_2O and diopside + dolomite + H_2O + CO_2 = tremolite + calcite (Fig. 6B).

At 20 kbar pressure, the assemblage becomes more stable by the reactions: calcite + diopside + H_2O + CO_2 = zoisite + dolomite; diopside + calcite = dolomite + quartz and dolomite + zoisite + CO_2 = diopside + calcite and show that with increasing pressure, the stability field shifts to higher temperature with higher X_{CO2} (Fig. 6C). Therefore, by considering Yei and Hirajima's results [46], the assemblage of zoisite + diopside +calcite + dolomite that formed in early stage of metamorphism could be stable at pressure at least higher than 8 kbar. Another fact for the high-pressure of the early stage of metamorphism comes from high Al-titanite. Although high Al-titanite was also reported in low-pressure rocks, it is closely associated with eclogite facies garnet and/or zoisite and is not a product of amphibolitization [40]. The octahedral Al-content in titanite has been shown to increase with pressure and to decrease with temperature in the fixed bulk chemical composition in the Ti-Al-Ca-Si-O-F system in the P-T range of 15-40 kbars and 1000-1200 ºC [40]. The high Al-titanite in the marble studied has a more than 40% replacement of Ti by Al, and no Fe^{3+} and almost reaches the extreme limit of replacement of Ti by Al in the octahedral chain of titanite, and it is associated with pure zoisite. Zoisite, itself, is also attributed to the eclogite facies, since its upper stability field is known to reach at least 35 kbar at 800 ºC and it coexists with high Al-titanite, and it exists in many non-retrogressed kyanite lineage eclogite [6]. Eventhough, the coexistence of high aluminum titanite, pure zoisite, jadeite-bearing diopside in early stage metamorphism of the studied marble implies high-pressure condition but up to now the pressure did not calibrate quantitatively. To consider the P-T-X_{CO2} stability of the observed mineral assemblage of the early and main stages of the metamorphism, we used the internally consistent thermodynamic dataset of Holland and Powell [24] and the THERMOCALC 3.21 software [36] by considering following assumptions for solid phase activities and metamorphic fluid fugacities. Following Holland and Powell [24], for clinopyroxene, the nonideality was considered to the set of end-members diopside (Di), Ca-tschermak(Cats), jadeite (Jd) and hedenbergite (Hd) with symmetric formalism interaction energies ($KJmol^{-1}$): W_{Di-Hd}=3, $_{WDi-Cats}$=7, W_{Di-Jd}=24, $W_{Hd-Cats}$=4, W_{Hd-Jd}=24, $W_{Cats-Jd}$=20. For amphiboles, the nonideality is approximated by renormalizing to the set of end-members tremolite (Tr), ferroactinolite (Fac), tschermakite (Ts) and glaucophane (Gln) with symmetric formalism interaction energies ($KJmol^{-1}$) (Dale et al. 2000): W_{Tr-Fac}=11.4, W_{Tr-Ts}=20.8, W_{Tr-Gln}=35.3, $W_{Fac-Gln}$=15, W_{Ts-Gln}=15. For the chlorite, the set of end-members clinchlore (Clc), daphinite (Dph) and amesite (Ame) was considered with nonideality arising with symmetric formalism intraction energies ($KJmol^{-1}$) [24]: $W_{Clc-Dph}$=2.5,$W_{Clc-Ame}$=18, $W_{Dph-Ame}$=20.5. For calcite, end-members of calcite (Cal), magnesite (Mgs), siderite (Sd) and rhodochrosite (Rds) with following intraction energies ($Kjmol^{-1}$) was considered [24]: $W_{Cal-Mgs}$=22, W_{Cal-Sd}=18, $_{WMgs-Sd}$=4. For dolomite, two end-members of dolomite (Dol) and ankerite (Ank) with intraction energy of 3 $KJmol^{-1}$ was considered. Powell and Holland [34,35] and Holland and Powell [25] introduced following equation to calculate fugacities and activities of metamorphic fluids in THERMOCALC software: $RTLn\ f_i=a + BT + CT^2$. They argue that the quality of the P-V-T data for C-O-H fluids at elevated temperature and presasure do not warrant a sophisticated equation of state and advocate that a polynominal fit to $RTlnf_i$ is adequate to model existing data. This procedure works fine as long as the same equations are used to calculate the thermodynamic equilibria at P and T that were used to extract the thermodynamic data in the first place. The tremendous advantage of such procedure is one of computational speed and its major disadvantage is that polynomial fits

are notoriously bad for extrapolations beyond the P and T of the original data [41]. However, because the equilibrated pressure and temperature of the marbles are extremely related to the amounts of fugacity and activity of metamorphic fluids, an alternate approach was used to calculate them. Here, we used following equation to calculate the fugacity of any component in the fluid mixture [41]:

$Lnfi(V,T)=Ln[\bar{V}_{mix}/V_{mix}b_{mix}]+[b_i/\bar{V}_{mix}b_{mix}][2X_ia_i+2\sum Xjaij/b_{mix}RT^{1.5}]+Ln[\bar{V}_{mix}+b_{mix}/\bar{V}_{mix}]+[a_{mix}b_i/(b_{mix})^2RT^{1.5}]Ln[(\bar{V}_{mix}+b_{mix}/\bar{V}_{mix})-(b_{mix}/\bar{V}_{mix}+b_i)]-ln(\bar{V}_{mix}/RT)+Ln(X_i)$

$\bar{V}_{mix}$ can be calculated in every pressure and temperature from the following equation:

$P=(RT/\bar{V}_{mix}-b_{mix})-[a_{mix}/T^{0.5}\bar{V}_{mix}(\bar{V}_{mix}+b_{mix})]$

In the Redlich-Kwong equation the term b refers to the volume occupied by the molecules themselves (the repulsive force) and is traditionally written for mixtures as a weighted average of the b coefficient for the individual molecules: $b_{mix}=\sum_{i=1}^{n} Xibi$

Where b_i and X_i are the b term and mole fraction of species and b_{mix} is the b coefficient for the mixture. In the Redlich-Kwong equation the term a refers to attractive forces that can be written in the form a(T) = å + a_1(T). In this equation å is a species dependent constant and a_1(T) is a polynominal in T. The term a_{ij} refers to dispersive forces for two nonpolar molecules and is written in the form $a_{ij}=\sqrt{å_i å_j}$ where $å_i$ and $å_j$ are the temperature dependent mixing terms. Equilibrium constant for the H_2O-CO_2 mixture can be computed by following equation:

$lnK=-11.7+(5953/T)-(2746*10^3/T^2)+(464.6*10^6/T^3)$

Finally, the term a_{mix} can be computed from the following equation: $a_{mix}=\sum_{i=1}^{n}\sum_{j=1}^{n} XjXia_{ij}$

By considering these assumption especially on fugacity of metamorphic fluids, the P-T-X_{CO2} estimates obtained using THRMOCALC show that the early stage mineral assemblage is stable between (P=12.8kbar, T=659 ºC, X_{CO2}=0.3) and (P=14.2kbar, T=684 ºC, X_{CO2}=0.4)(Fig. 7). The P-T-X_{CO2} calculation by THERMOCALC for the main stage mineral assemblage indicates that this stage is stable between (P=3.3 kbar, T=489 ºC, X_{CO2}=0.5) and (P=4.4 kbar, T=511 ºC, X_{CO2}=0.4) (Fig. 7).

Assuming that the maximum pressure (14.2kbar) recorded by the marble is due exclusively to the lithostatic pressure, we estimated that the marbles from the Nahavand area reached depths of at least 60 km, corresponding to a geothermal gradient of almost 10-12 ºC/km that is consistent with metamorphism in a subduction zone. Thermobaric calculations show a nearly retrograde decompressive path from an amphibole-eclogite to greenschist facies conditions (Fig. 7). Many subduction P-T paths show a generally clockwise loop where high-pressure and low-temperature subduction metamorphism is followed by decompression. The metamorphic consequence of this P-T trajectory is extensive greenschist or amphibolite facies overprint on the early blueschist or eclogite facies metamorphism that has been named western Alpine type subduction metamorphism [14]. In the studied marbles, also an early stage eclogite facies mineral assemblage undervent a marked greenschist facies overprint that is closely consistent with the western Alpine subduction metamorphism. Therefore, the relatively high-pressure mineral assemblage in marbles from north of the Nahavand area indicates that this assemblage could be formed during subduction of the Neo-Tethys oceanic plate under the Iranian microcontinent. Such an interpretation is in agreement with Berberian and King [5], Alavi[2], Mohajjel et al. [32], Ghasemi and Talbot [18] and Davoudian et al. [12] conclusions.

Acknowledgement

We are most thankful to the University of Zanjan for the financial support of this study. The authors also thank the reviewers for their constructive comments and editorial efforts.

References

1. Agard P., Monié P., Gerber W., Omrani J., Molinaro M., Meyer B., Laborousse L., Vrielynck B., Jolivet L. and Yamato P. Transient, synobduction exhumation of Zagros blueschists inferred from P-T, deformation, time, and kinematic constraints: Implications for Neotethyan wedge dynamics. *J. Geophic. Res.* **111**: 1-28 (2006).
2. Alavi M. Tectonics of the Zagros orogenic belt of Iran: new data and interpretations. *Tectonophysics* **229**: 211-238 (1994).
3. Alavi M. and Mahdavi M.A. Stratigraphy and structure of the Nahavand region in western Iran and their implications for the Zagros tectonics. *Geol. Mag.* **131**: 43-47 (1994).
4. Armstrong J.T. Quantitative analysis of silicates and oxide minerals: comparison of Monte-Carlo, ZAF and Phi-Rho-Z procedure. *Microbeam Analysis* 239-246 (1988).
5. Berberian M. and King G.C. Towards a paleogeography and tectonics evolution of Iran. *Can. J. Earth Sci.* **18**: 210-265(1981).
6. Bohlen S.R. and Boettcher A.L. The quartz-coesite transformation: a pressure determination and effects of other composition. *J. Geophic. Res.* **87**: 7073-7078 (1982).
7. Carswell D.A. *Eclogite facies rocks*. Blackie and Son Ltd, 552p. (1990).
8. Castelli P. Il metamorfismo alpino della rocce carbonatiche

della zona Sesia Lanzo (Alpi Occidentali). Ph.D. *Thesis*, Universita di Torino, 141p (1987).
9. Compagnoni P. The Sesia-Lanzo zone: high pressure–low temperature metamorphism in the Austroalpine continental margin. *Rend. Soc. Ital. Mineral. Petrol.* **33**: 335-374 (1977).
10. Dachs E. High-pressure mineral assemblages and their breakdown products in metasediments, south-central Tauern window, Austria. *Chem. Geol*. **50**: 33-46 (1986).
11. Dale J., Holland T.J.B. and Powell R. Hornblende-garnet-plagioclase thermobarometry: a natural assemblage calibration of the thermodynamics of hornblende. *Contrib. Mineral. Petrol.* **40**: 353-362 (2000).
12. Davoudian A.R., Genser J., Dachs E. and Shabanian N. Petrology of eclogite from north of Shahrekord, Sanandaj-Sirjan zone, Iran. *Mineral. Petrol.* **92**: 393-413 (2008).
13. Ernst W.G. Coexisting sodic-calcic amphiboles from high-pressure metamorphic belts and the stability of barroisitic amphiboles. *Mineral. Mag.* **43**: 269-278 (1979).
14. Ernst W.G. Tectonic history of subduction zones inferred from retrograde blueschist P-T paths. *Geology* **16**: 1081-1084 (1988).
15. Ernst W.G. Preservation/exhumation of ultrahigh-pressure subduction complexes. *Lithos* **92**, 321-335 (2006).
16. Franz G. and Spear F.S. High pressure metamorphism in siliceous dolomites from the central Tauern window, Austria. *Ame. J. Sci.* **283(A)**: 396-413 (1983).
17. Franz G. and Spear F.S. P-T evolution of metasediments from the Eclogite zone, south-central Tauern window, Austria. *Lithos* **19**: 219-234 (1985).
18. Ghasemi A., and Talbot C. A new tectonic scenario for the Sanandaj-Sirjan Zone (Iran). *J. Asian Earth Sci*. **26**: 683-693 (2006).
19. Heinrich C.A. Eclogite facies regional metamorphism of hydrous mafic rocks in the central alpine Adula nappe. *J. Petrol.* **27**: 123-124 (1986).
20. Heinrich H. and Althaus E. Experimental determination of the 4 lawsonite + albite = paragonite + 2zoisite + 2quartz + $6H_2O$. *Neues Jahrbuch für Mineralogie Monatshefte* **11**: 516-528 (1988).
21. Holdaway M.J. Stability of andalusite and the aluminium silicate phase diagram. *Am. J. Sci*. **271**: 97-131(1971).
22. Holland T.J.B. Experimental determination of the reaction paragonite = jadeite + kyanite + H_2O, and internally consistent thermodynamic data for part of the system Na_2O-Al_2O_3-SiO_2-H_2O, with applications to eclogites and blueschists. *Contrib. Mineral. Petrol.* **68**: 293-301(1979).
23. Holland T.J.B. The reaction albite = jadeite + quartz determined experimentally in the range 600-1200°C. *Am. Mineral.* **65**: 129-134(1980).
24. Holland T.J.B. and Powell R. An internally consistent thermodynamic data set for phases of petrological interest. *J. Metamorph. Geol.* **16**: 309-343 (1998).
25. Holland T.J.B. and Powell R. An internally-consistent thermodynamic dataset with uncertainties and correlations: the system Na_2O-K_2O-CaO-MgO-MnO-FeO-Fe_2O_3-Al_2O_3-SiO_2-TiO_2-C-H_2-O_2. *J. Metamorph. Geol.* **8**: 89-124(1990).
26. Hsu L.C. Selected phase relationships in the system Al-Mn-Si-O-H: a model for garnet equilibria. *J. Petrol.* **9:** 40-83 (1968).
27. Izadyar J., Mojab S., Kuroshi O. and Zare M. An unusuall assemblage of talc-phengite-chlorite-K-feldspar in quartz schists from the Nahavand area, Sanandaj-Sirjan zone, Iran. *Iranian J. Sci. and Technol.* **38**: 243-252 (2014).
28. Izadyar J., Mousavizadeh M. and Eram M. Metamorphic evolution of high-pressure quartz schists in the Chadegan metamorphic complex, Sanandaj-Sirjan zone, Iran. *J. Geopersia* **2**: 1-20 (2013).
29. Leake B.E., Woolley A.R., Arps C.E.S., Birch W.D., Gilbert M.C., Grice J.D., Hawthorne F.C., Kato A., Kisch H.J., Krivovichev V.G., Linthout K., Laird J., Mandarino J. M., Maresch W.V., Nickel E.H., Rock N.M.S., Schmacher J.C., Smith D. C., Stepehnson N.C.N., Ungaretti L., Whittaker E.J.W. and Youzhi G. Nomenclature of amphiboles: Report of the subcommittee on Amphiboles of the International Mineralogical Association on New Minerals and Mineral Names. *Am. Mineral.* **82**: 1019-1037 (1997).
30. Matthews A. and Schliestedt M. Evolution of the blueschsit and greenschistfacies rocks of Sifnos, Cyclades, Greece. A stable isotope study of subduction related metamorphism. *Contrib. Mineral. Petrol.* **88**: 150-163 (1984).
31. Mohajjel M. and Fergusson C. L. Dextral transpression in Late Cretaceous continental collision, Sanandaj-Sirjan Zone, western Iran. *J. Struct. Geol.* **22**: 1125-1139 (2000).
32. Mohajjel M., Fergusson C.L. and Sahandi M.R. Cretaceous-Tertiary convergence and continental collision, Sanandaj-Sirjan Zone, western Iran. *J Asian Earth Sci.* **21**: 397-412 (2003).
33. Pognante U., Talarico F., Rastelli N. and Ferrati N. High pressure metamorphism in the nappes of the valledell'Orco traverse (western Alps). *J. Metamorph. Geol.* **5**: 397-414 (1987).
34. Powell R. and HollandT.J.B. An internally consistent thermodynamic dataset with uncertainities and correlations: 1, Methods and worked example. *J. Metamorph. Geol.* **3**: 327-342 (1985).
35. Powell R. and Holland T.J.B. An internally consistent dataset with uncertainities and correlations: 3. Aplications to geobarometry, worked examples and a computer program. *J. Metamorph. Geol.* **6**: 173-204 (1988).
36. Powell R., Holland T.J.B. and Worley B. Calculating phase diagrams with THERMOCALC: methods and examples. *J. Metamorph. Geol.* **6**: 173-204 (1998).
37. Plyusnina L.P. Geothermometry and geobarometry of plagioclase-hornblende-bearing assemblage. *Contrib. Mineral. Petrol*. **80**: 140-146 (1982**)**.
38. Şengör A.M.C. The cimmeride orogenic system and the tectonics of Eurasia. *Geolic. Soci. Am. Special Paper* 195 (1984).
39. Şengör A.M.C. and Natal'in B.A. Paleotectonics of Asia: fragments of a synthesis. In: Yin A., and Harrison T.M., (Eds.), *The tectonics evolution of Asia*, Cambridge University Press, pp. 486-640 (1996**)**.
40. Smith D.C. A review of the peculiar mineralogy of the Norwegian coesite-eclogite province with crystal-chemical petrological and geodynamical notes and an extensive bibliography. In: Smith D.C.(Ed.), *Eclogites and eclogite facies rocks*. Elsevier, New York, pp. 1-178 (1988).
41. Spear F.S. *Metamorphic phase equilibria and pressure-*

temperature-time paths. Mineralogical Society of America, Washington, (1990).
42. Spear F.S. and Franz G. P-T evolution of metasediments from the eclogite zone, south-central Tauern window, Austria. *Lithos* **19**: 219-234 (1986).
43. Stöclin J. Structural history and tectonics of Iran: a review. *Am. Associ. Petroleum Geol. Bull.* **52**: 1229-1258 (1968).
44. Vielzeuf D. and Holloway J.R. Experimental determination of the fluid-absent melting relations in the pelitic system. *Contrib. Mineral. Petrol*. **98**: 257-276 (1988).
45. Vielzeuf D. and Schmidt M. Melting relations in hydrous system revisited: application to metapelites, metagreywackes and metabasalts. *Contrib. Mineral. Petrol.* **141**: 251-267 (2001).
46. Ye K. and Hirajima T. High-pressure marble at Yangguantun, Rongchengcounty, Shandong province, eastern China. *Mineral. Petrol.* **57**: 151-165 (1996).
47. Whitney D.L. and Evans B.W. Abbreviations for names of rock-forming minerals. *Am. Mineral.* **95**: 185-187 (2010).